International Journal of Machine Tools & Manufacture 50 (2010) 115–125

Contents lists available at ScienceDirect

International Journal of Machine Tools & Manufacture

journal homepage: www.elsevier.com/locate/ijmactool

Laser polishing of tool steel with CO_2 laser and high-power diode laser

Ukar E.[a,*,1], Lamikiz A.[a,1], López de Lacalle L.N.[a,1], del Pozo D.[b,2], Arana J.L.[a,1]

[a] *Department of Mechanical Engineering, University of the Basque Country, ETSII, c/Alameda de Urquijo s/n, 48013 Bilbao, Spain*
[b] *Robotiker Technology Centre, Parque Tecnológico, Edif. 202, Zamudio 48170, Spain*

Laser polishing

DIN 1.2379 tool steel

Laser

CO2 Laser **Diode Laser**

Surface process methods

Milling **EDM**

1. Introduction

Finishing operations on large metallic surfaces constitute major processes within the die and mold industry. At present the final polishing operation is carried out manually, and this accounts for more than 20% of total manufacturing time for the entire mold or stamping die. Moreover, the process must be carried out by highly qualified workers, leading to high production costs and long lead times.

This paper focuses on application of the laser-polishing process on milled and EDMed metallic surfaces of medium-to-large dimensions, such as die and mold surfaces. An in-depth analysis of the effect of laser radiation on the metallurgical structure of DIN 1.2379 tool steel is presented too. The discussion of experimental results takes into account not only the roughness reduction rate, but also the thermal impact on the surface material. Thus there is also evaluation of a potential mechanical behavior change, which must be considered in order to obtain the functional requirements of dies and molds.

Since the ultimate aims of the work set out in this paper were the industrial application of the laser-polishing process and its effect on part integrity, the study focused on industrial CO_2 and high-power diode lasers in CW continuous-wave mode, those most commonly used in industrial environments. Many mold manufacturers, in fact, use these types of laser for cutting or tempering applications.

2. Experimental setup

In order to evaluate the influence of the parameters and the type of laser on the surface roughness results, laser-polishing tests were carried out on milled and EDMed surface using two different industrial laser types: a 3100 W ROFIN DL 031Q diode laser guided by a FANUC S-10 robot, and a 2500 W CO_2 ROFIN DC025 slab laser in a 3-axis gantry structure with a maximum feed rate of 10,000 mm/min. Spot size in the diode laser is a rectangular shape 1.2 × 2 mm with a 906 nm wavelength, while the CO_2 laser has a Ø 0.8 mm circular spot on the focal point with a 10,600 nm wavelength.

One of the key parameters in the process is the energy distribution of the laser spot. Each type of laser has a different type of energy distribution. CO_2 lasers usually present a Gaussian energy distribution, whereas a diode laser presents a top-hat distribution.

The surface topographies present a pattern of peaks and valleys, and their frequency and amplitude set the quality of the surface, usually expressed as roughness. Roughness can be measured using different parameters, depending on the physical characteristic measured. In the die and mold industry, for example, roughness is evaluated using three different parameters—*Ra*, *Rz* and *Rt*.

The tests were measured with a Taylor Hobson profilometer that can measure both roughness and profile in 2D and 3D. Due to the natural random nature of surface roughness, three different parameters were employed for each polishing test: the mean roughness (*Ra*), average maximum height of the profile (*Rz*) and maximum height of the profile (*Rt*). Using these *Ra*, *Rz* and *Rt* values, it is possible to define the percentage reduction of each parameter that indicates the reduction ratio obtained with respect to the initial roughness value. Moreover, in order to obtain a precise value, three different roughness measurements were taken for each test.

2. Laser polishing test with CO2 and diode laser

The polishing tests were carried out on a planar surface topography generated by milling with a Ø 16 mm ball-end mill and a 1.5 mm radial depth of cut. This surface may be considered as a typical semi-finished surface in the die and mold industry. It has been observed in previous works [9] that, as the initial surface roughness decreases, the laser-polishing process is less effective. In other words, the better the initial surface finish, the lower the polishing rates for the laser process. The reference topography, therefore, is a semi-finished surface, which also entails greater cost savings, since there is no need for a finishing milling operation.

The tests consisted of a series of individual polishing test lines on a semi-finished planar surface. The test lines, 20 mm in length, were carried out at a 45° angle with respect to the milling direction, as may be observed in the test part shown in Fig. 2.

Once the test part had been designed and milled, a set of linear polishing tests were carried out with both the CO_2 and diode lasers. As mentioned above, a DoE methodology was employed and the same initial surface used in all tests. The roughness parameters of the initial surface are: 5.32 µm *Ra*, 24.93 µm *Rz* and 25.63 µm *Rt*.

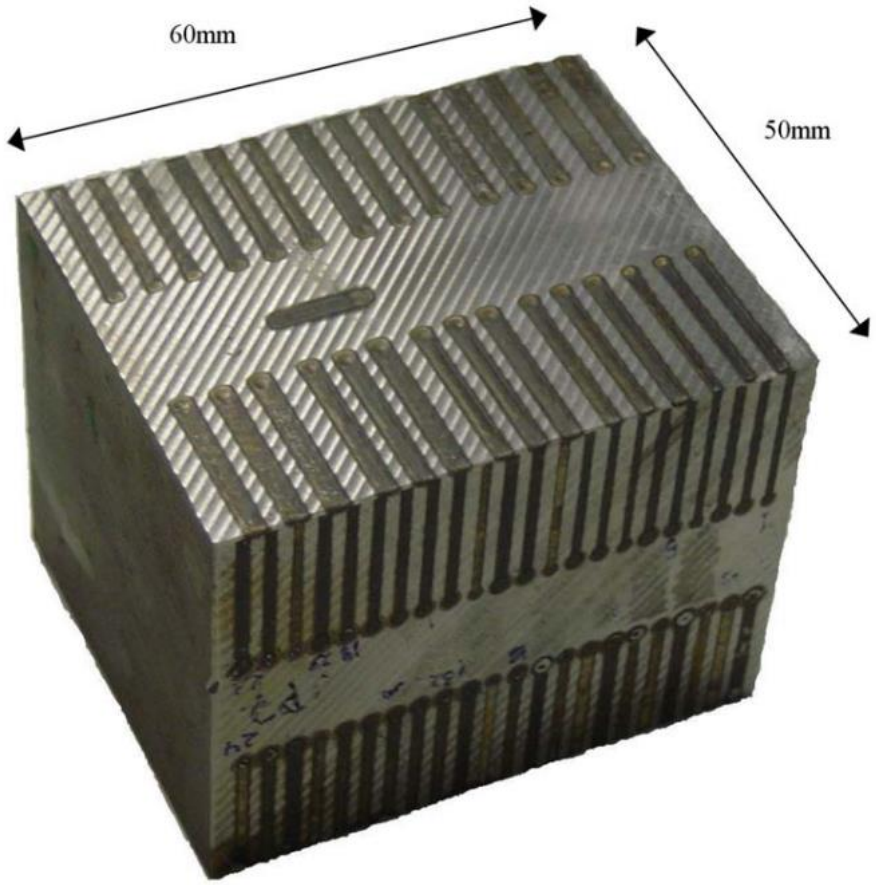

2. Laser polishing test with CO2 and diode laser

In order to set the parameter magnitude range for the DoE, a series of preliminary tests were carried out, in which minimum and maximum energy densities for each laser type were defined. For the minimum energy value the material is practically unmelted, and for maximum value an SOM regime was clearly observed. Nevertheless, due to the wavelength difference of each laser type (906 nm for the diode laser and 10,600 nm for the CO_2 laser), the amount of energy absorbed by the material is not the same for the two laser types. Thus different parameter magnitude ranges were obtained for each type.

When the polished surface area per time unit is also taken into account, the productivity of the diode laser is clearly higher than that obtained with the CO_2 laser. Since the spot has a width of

with less energy density in the diode laser than in the CO_2 laser. This difference is caused mainly by the material's energy absorption, which is much higher for the diode laser beam wavelength.

2. Laser polishing test with CO2 and diode laser

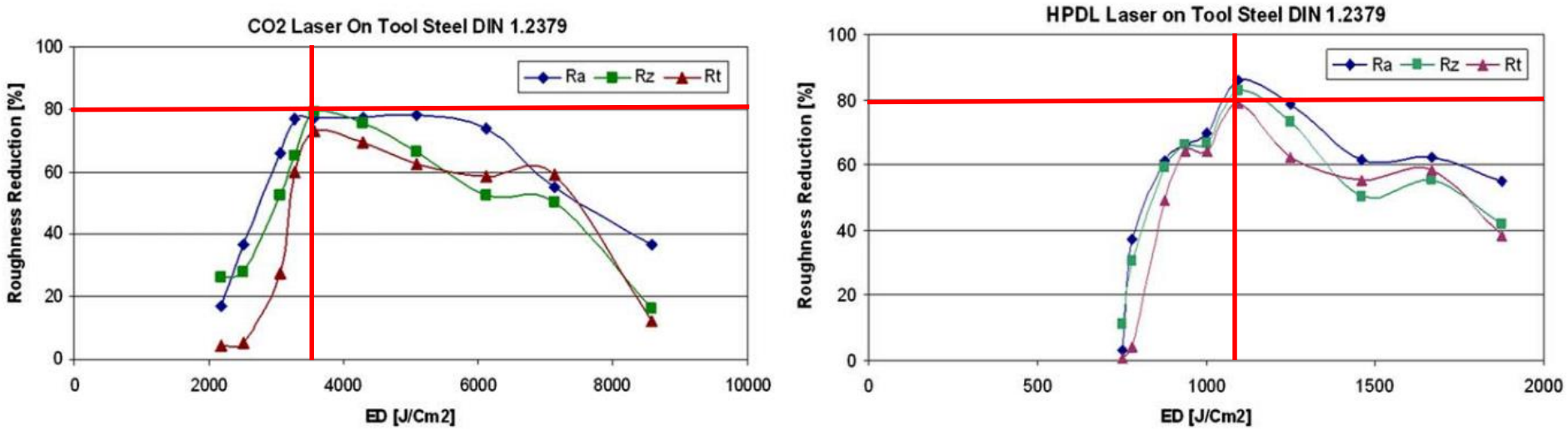

Fig. 4. Energy density and roughness reduction rate with CO_2 laser (left) and HPDL (right) on DIN 1.2379 tool steel.

Fig. 4 shows the trend in the roughness reduction rate in accordance with the energy density for both laser types.

Considering the results obtained with the DoE methodology, the laser-polishing process achieves a considerable roughness reduction, up to 85% with respect to the initial roughness values, with *Ra* values below 1 µm, the value typically considered for a polished surface in the die and mold industry.

2. Laser polishing test with CO2 and diode laser

One of the most relevant conclusions of the DoE tests is the superior result of the diode laser with respect to the CO_2 laser. In order to complete the analysis obtained on the previous laser-polishing test, a new set of individual polishing tests were drawn up for the diode laser, with the same initial surface, milled with a Ø 16 mm ball-end mill and a radial step of 1.5 mm. In this case, however, the power parameter was increased linearly in order to obtain a full range of energy density and evaluate the influence of this parameter from very low values up to extremely high energy densities.

Moreover, the tested material (DIN 1.2379 tool steel) was maintained, although in this case the polishing tests were carried out perpendicular to the milling pattern. Although this change introduces a modification to polishing strategy, the results obtained from this second group of tests show that there is no variation with respect to the initial tests. In other words, no influence of the polishing strategy on final roughness reduction was observed. In this case, the initial roughness values were measured perpendicular to the milling direction, producing initial values of *Ra*=7.07, *Rz*=30.87 and *Rt*=31.6 µm, greater values than in previous tests.

Table 3
Tested parameters and results for laser-polishing process increasing linearly the energy density on DIN 1.2379 tool steel with diode laser.

Run	Power (W)	Feed Rate (mm/min)	Spot Width (mm)	ED (J/cm²)	Initial Values			Final Values					
					Initial Ra (µm)	Initial Rz (µm)	Initial Rt (µm)	Ra (µm)	Rz (µm)	Rt (µm)	Ra Red. (%)	Rz Red. (%)	Rt Red. (%)
1	250	1920	2	390.6	7.07	30.87	31.60	–	–	–	–	–	–
2	300			468.8				–	–	–	–	–	–
3	350			546.9				6.23	24.43	25.50	11.88	20.86	19.30
4	400			625				5.55	23.03	28.70	21.50	25.40	9.18
5	450			703.1				3.22	15.33	18.30	54.46	50.34	42.09
6	500			781.3				3.16	14.27	14.60	55.30	53.77	53.80
7	550			859.4				2.12	11.37	12.50	70.01	63.17	60.44
8	600			937.5				2.15	12.44	13.66	69.59	59.70	56.77
9	650			1015.6				1.97	10.60	14.08	72.14	65.66	55.44
10	700			1093.8				1.37	9.19	10.59	80.62	70.23	66.49
11	750			1171.9				0.86	4.69	7.68	87.84	84.81	75.70
12	800			1250				1.39	10.40	11.40	80.34	66.31	63.92
13	850			1328.1				1.82	10.06	11.40	74.26	67.41	63.92
14	900			1406.3				1.94	10.66	13.80	72.56	65.47	56.33
15	950			1484.4				2.14	15.10	16.40	69.73	51.09	48.10
16	1000			1562.5				2.32	14.73	16.30	67.19	52.28	48.42
17	1050			1640.6				1.93	13.17	14.10	72.70	57.34	55.38
18	1100			1718.8				1.89	10.76	12.40	73.27	65.14	60.76
19	1150			1796.9				1.87	12.13	16.7	73.55	60.71	47.15
20	1200			1875				1.65	13.57	21.4	76.66	56.04	32.28
21	1250			1953.1				1.74	14.13	22	75.39	54.23	30.38
22	1300			2031.3				1.92	15.30	24.00	72.84	50.44	24.05

2. Laser polishing test with CO2 and diode laser

The results of the tests shown in Fig. 5 demonstrate a roughness improvement if energy density increases, up to a maximum reduction rate of 87% *Ra*, corresponding to 1100 J/cm^2. These results are similar to those obtained in the previous tests. Once this maximum roughness reduction is achieved, if energy density is increased, roughness reduction decreases. This trend would again appear to perfectly match the transition from SSM to SOM regime.

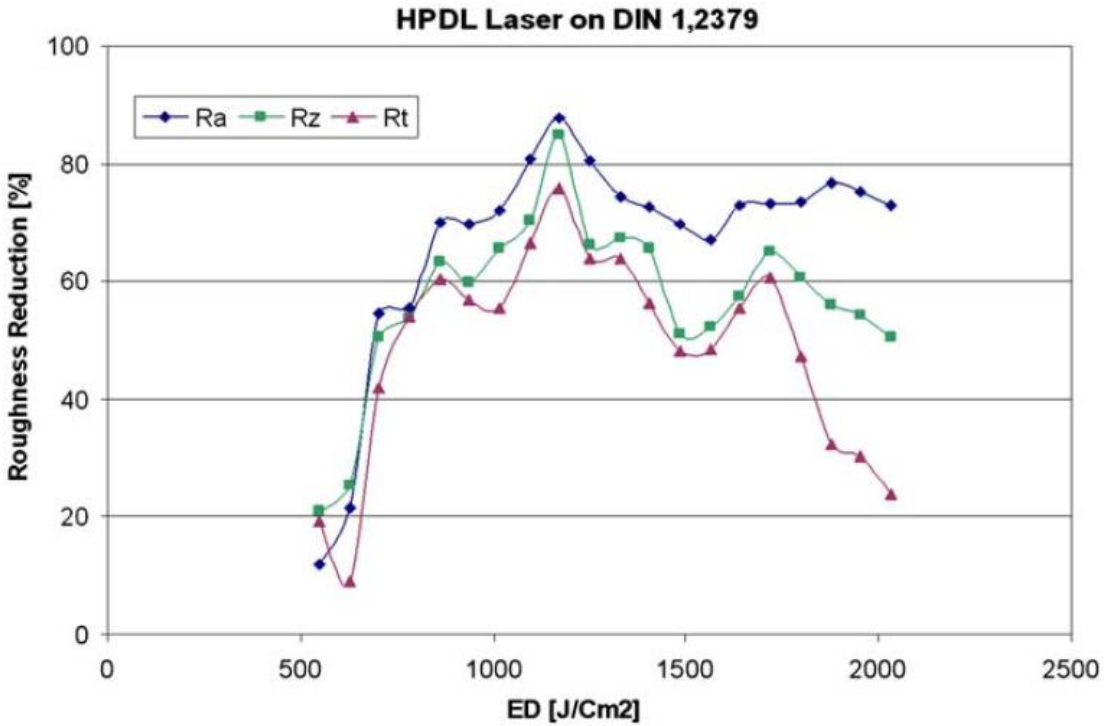

Fig. 5. Roughness reduction rates—*Ra*, *Rz* and *Rt* roughness parameters for tested energy densities.

2. Laser polishing test with CO2 and diode laser

Run	Power (W)	Feed Rate (mm/min)	Spot Width (mm)	ED (J/cm²)	Initial Values			Final Values					
					Initial Ra (µm)	Initial Rz (µm)	Initial Rt (µm)	Ra (µm)	Rz (µm)	Rt (µm)	Ra Red. (%)	Rz Red. (%)	Rt Red. (%)
1	250	1920	2	390.6	7.07	30.87	31.60	–	–	–	–	–	–
2	300			468.8				–	–	–	–	–	–
3	350			546.9				6.23	24.43	25.50	11.88	20.86	19.30
4	400			625				5.55	23.03	28.70	21.50	25.40	9.18
5	450			703.1				3.22	15.33	18.30	54.46	50.34	42.09

measured perpendicular to the milling direction, producing initial values of *Ra*=7.07, *Rz*=30.87 and *Rt*=31.6 µm, greater values than

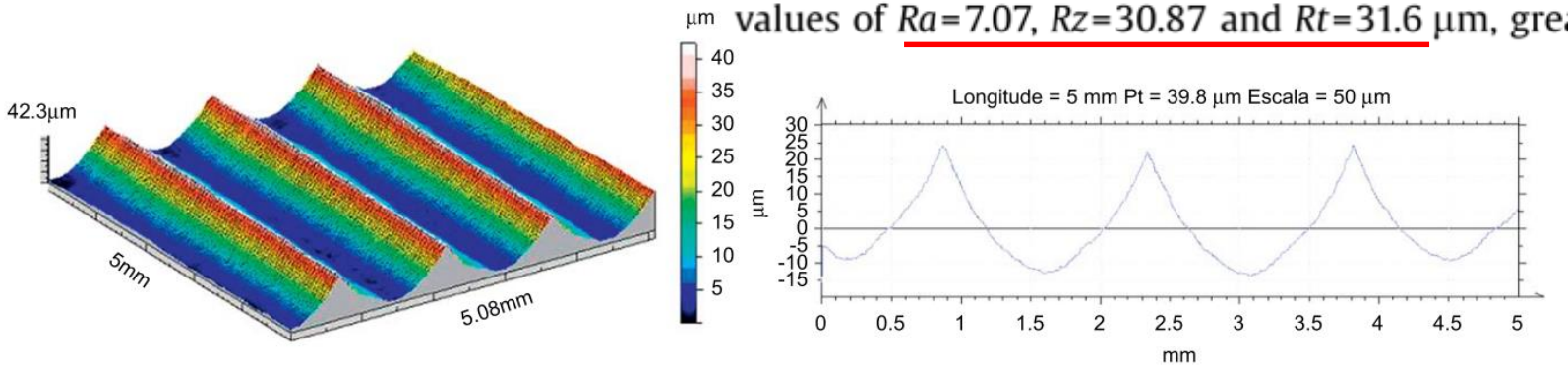

Fig. 6. Initial surface 3D topography (left) and extracted 2D profile (right).

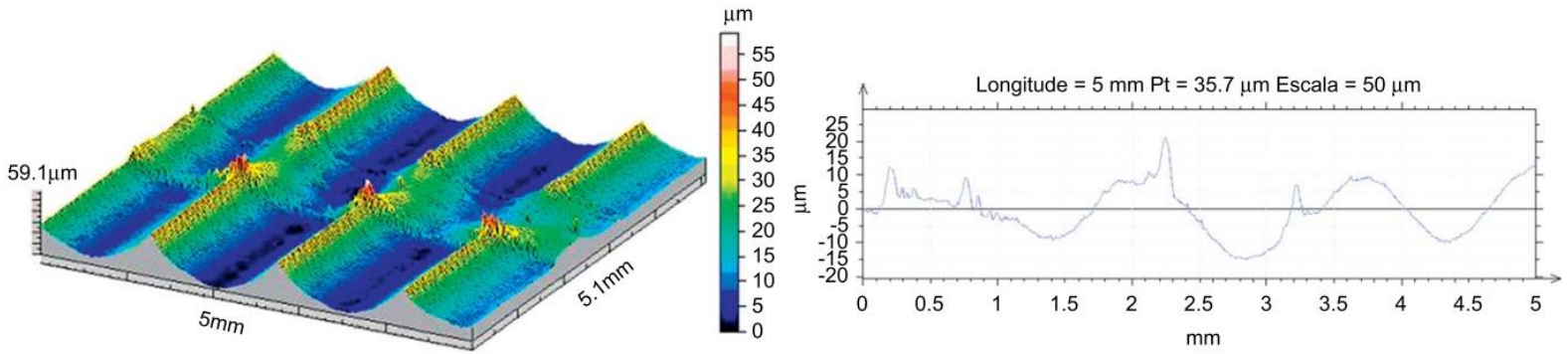

Fig. 7. 3D topography of run 4: low energy density test. *P*=400 W, Vf=1,920 mm/min, ED=625 J/cm2, Ra=5.55 µm, Rz=23.03 µm, Rt=28.7 µm.

2. Laser polishing test with CO2 and diode laser (ball-end mill)

Once the maximum roughness reduction is achieved, if energy density is increased the melted layer thickness becomes too great and material melt pool shows convective currents. Fig. 9 shows

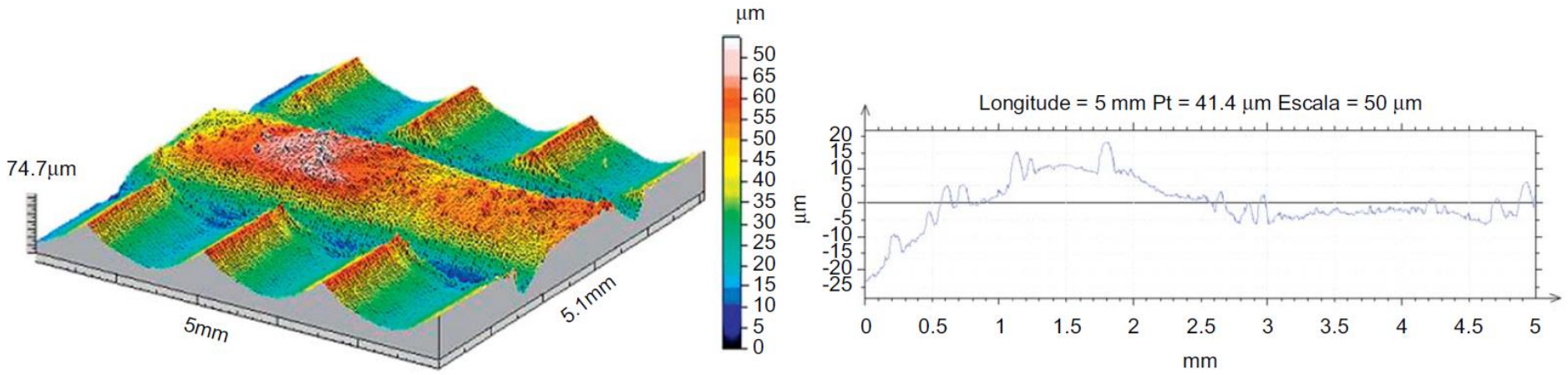

Fig. 9. 3D topography measured on a high energy density test (run 15 in Table 3). P=950 W, Vf=1,920 mm/min, ED=1,484 J/cm^2, Ra=2.14 µm, Rz=15.10 µm, Rt=16.40 µm.

2. Laser polishing test with CO2 and diode laser (ball-end mill)

Once the roughness parameters of the various tests had been studied, a metallurgical analysis of the tests was carried out in order to ensure surface integrity. It must be taken into consideration that both regimes, SSM and SOM, involve material melting, and therefore lower hardness and a heat-affected zone (HAZ) are expected.

The micro-structure analysis was carried out using the *Bechet-Beaujard* etchant process. Fig. 10 shows four different zones in the structure of each polishing test. *Zone A* indicates the area where the material has melted and resolidified. *Zone B* is a heat-affected zone where the melting temperature of 1600 °C has not been reached but temperature has risen over 723 °C. The limit of 723 °C corresponds to the A_1 transformation from pearlite to austenite for carbon steels with 1.5% C, as indicated in the carbon steel phase diagram, and thus there is metallurgical transformation in this area. The area defined as *Zone C* corresponds to the material where the temperature reached is below austenitizing temperature and the material is annealed, reducing its hardness by 10%.

Finally, the typical martensite structure may be observed in *Zone D* (base material), with small grain and chromium carbides, a typical structure of DIN 1.2379 tool steel with a high chromium content.

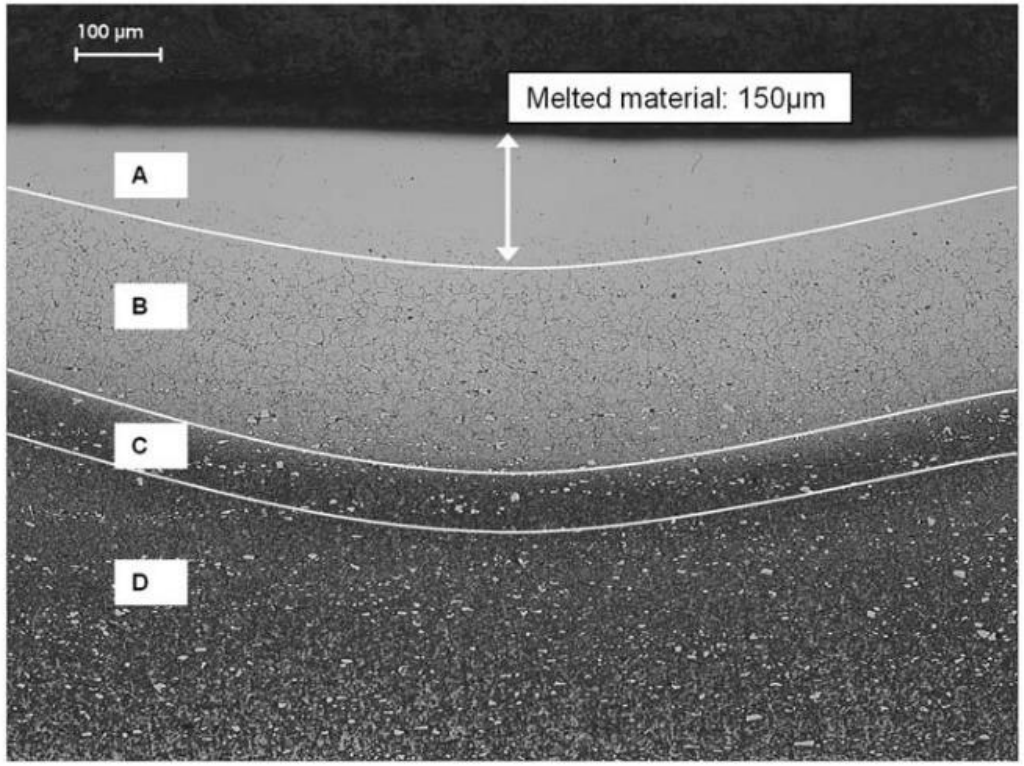

Fig. 10. Metallography structure of an optimum energy density test (run 4 in Table 3).

2. Laser polishing test with CO2 and diode laser (ball-end mill)

Fig. 11 shows the micro-hardness values for the optimum parameters where a roughness reduction of 85% of *Ra* has been obtained (run 11 in Table 3). In the analysis 21 hardness measurements were performed every 35 µm. Results are shown on the Rockwell C hardness scale (HRC), and the initial hardness for DIN 1.2379 tool steel is 62 HRC. Plotting the measured hardness as a function of the depth (µm) shows the hardness variation between the abovementioned zones. This hardness variation is shown in Fig. 12.

Zone A, corresponding to the melted layer, shows a thickness of 200 µm (indentation 7). Zone B, where hardness reaches the initial 62 HRC, starts from indentation 7–17, representing a layer thickness of 350 µm. Zone C, which is 100 µm thick, shows a hardness reduction of up to 54 HRC. Finally, Zone D shows the expected hardness again to the initial value of 62 HRC.

Similar results to those shown in Fig. 12 were obtained for all tests. Hardness reduction increases even more as the melt pool increases, and this depends on energy density.

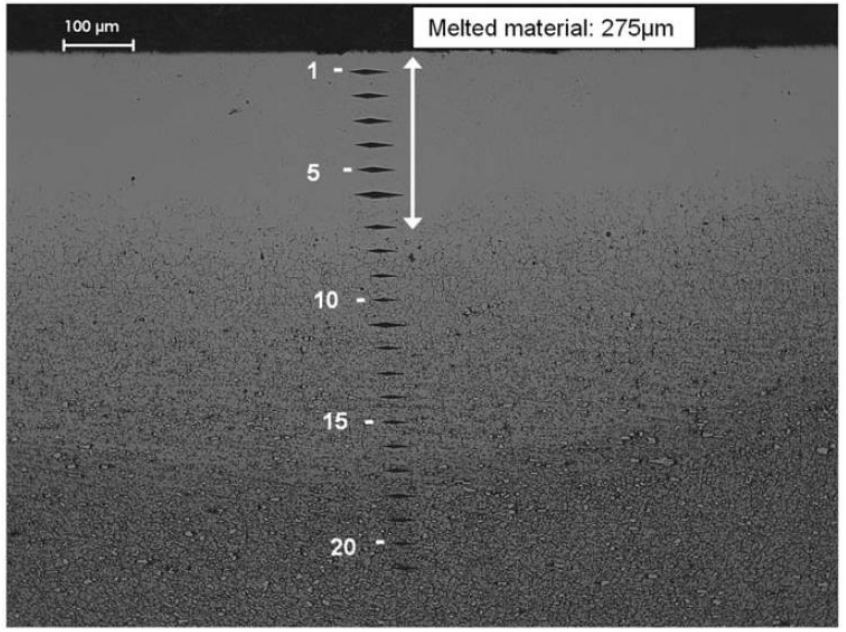

Identation	Depth (µm)	HRC
1	30	41,5
2	65	45,5
3	100	43,3
4	135	43,3
5	170	43,2
6	205	42,1
7	240	51,1
8	275	57,8
9	310	61,8
10	345	62,5
11	380	58,6
12	415	61,8
13	450	61,7
14	485	61
15	520	61,7
16	555	61,7
17	590	59,9
18	625	55,2
19	660	59
20	695	62,1
21	730	62,1

Fig. 11. Micro-hardness study on run 11 in Table 3.

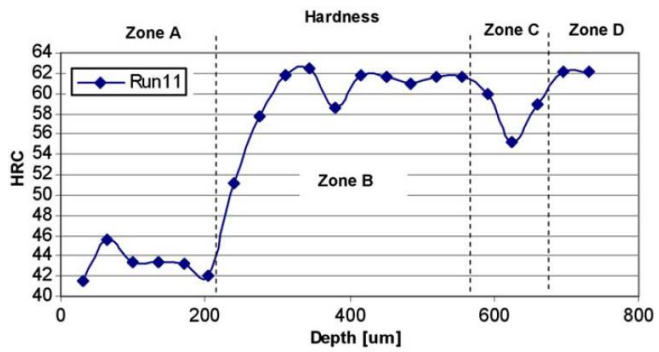

Fig. 12. Hardness trend after polishing on run 11 in Table 3.

2. Laser polishing test with CO2 and diode laser (ball-end mill)

Finally, using a Scanning Electron Microscope (SEM) some micro-cracks were detected when energy density was greater than 1250 J/cm^2. DIN 1.2379 tool steel is a cold work steel, and there is a risk of cracking if the thermal gradient is high. Although the laser beam effect is quite localized, the thermal gradient is extremely high, introducing thermal stress. Fig. 14 shows the micro-crack detected with an energy density of 1328 J/cm^2 (run 13 in Table 3). Although a micro-crack in itself does not alter the mechanical properties of the part, it can lead to the propagation of larger cracks when the part is under stress in service, mainly if variable stress or impacts are present. In this case, fatigue failure can be accelerated by these micro-cracks on the surface area. Energy density, therefore, must be limited not only due to roughness parameters, but also to reduce the risk of cracking.

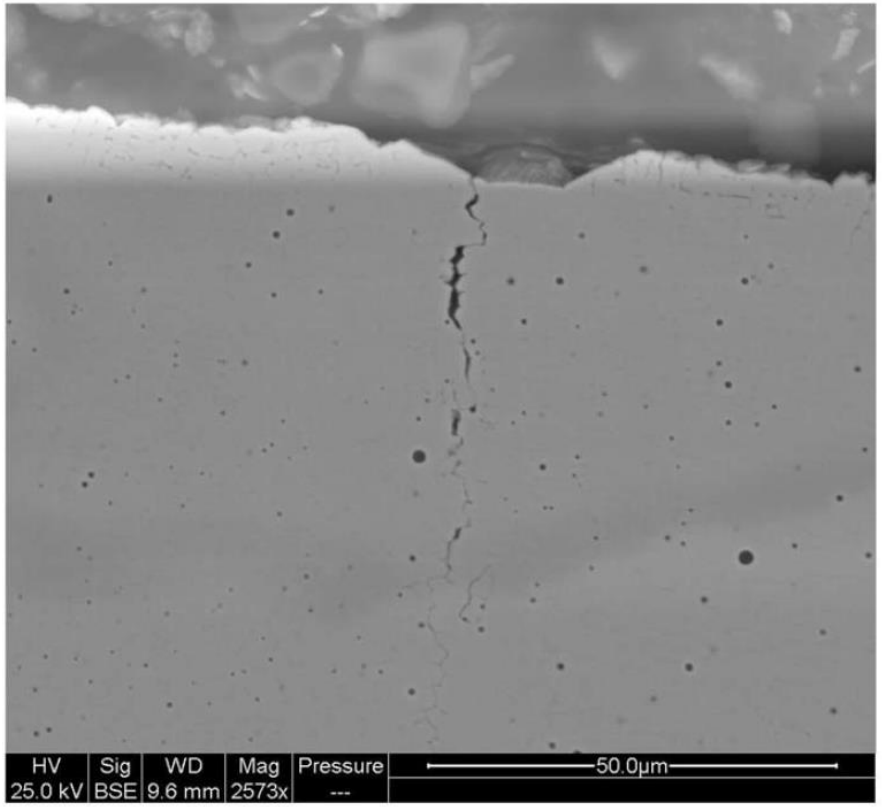

Fig. 14. Micro-crack with an energy density of 1328 J/cm^2.

3. Laser polishing test with diode laser on EDM finished surface

VDI33 obtained by the EDM process. This kind of surface presents a high frequency peak distribution with a lower *Ra* parameter than the milled surface, but with similar peak-to-valley distance, as may be observed in Fig. 15. The initial roughness parameters in this case are: *Ra*=4.4, *Rz*=21.8 and *Rt*=29.5 µm. Another relevant characteristic of this topography is that the peak and valleys are randomly distributed.

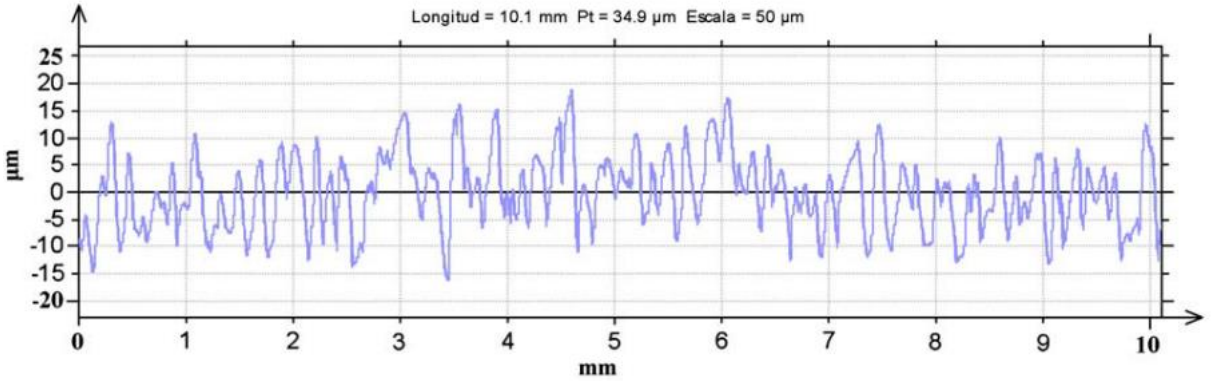

Fig. 15. Initial topography profile for the EDMed surface for VDI33 parameters.

distance between them, the best result was obtained with a remarkable lower energy density of 468 J/cm^2, using power 300 W and feed rate 1920 mm/min. Fig. 16 shows the result of the optimum test on the EDMed surface. The final surface roughness parameters with the optimum conditions are: *Ra*=0.36, *Rz*=2.61 and *Rt*=3.71 µm. This means a reduction of 91% *Ra*, 88% *Rz* and 87% *Rt*.

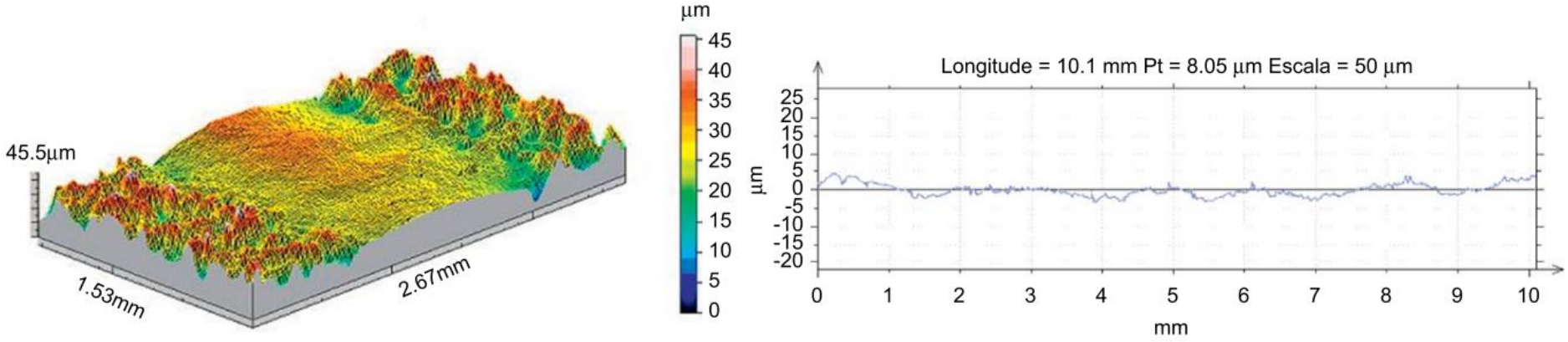

Fig. 16. 3D topography (left) and 2D profile (right) of the laser-polished area.

3. Laser polishing test with diode laser on EDM finished surface

As may be observed in Fig. 18, the hardness trend shows the same four different zones as in the results for Section 3.2. The melted layer depth in this case is below 35 µm, which is approximately the peak–valley distance (Rt=29.5 µm), and it shows a hardness of 54 HRC, which represents a reduction of 13% when compared with the initial hardness of 62 HRC. On the other hand, in Zone B, temperature reached the austenitizing temperature of 723 °C, though melting temperature was not attained. As temperature approaches the melting point, grain size is greater and hardness is lower. As may be observed in Figs. 17 and 18, hardness varies between 54 HRC and 62 HRC, as the measure indentation is deeper in Zone B. Although the hardness reduction is 13% when compared with the initial hardness of 62 HRC, hardness of 54 HRC is still high enough for most die and mold applications, and since the melted layer is below 35 µm, there will be no significant alterations of mechanical properties from a macroscopic point of view. Moreover, in this case no crackings or inclusions were detected.

As may be observed in Table 4, the maximum reduction is obtained for a melted layer thickness similar to the average peak–valley distance. Nevertheless, for energy density values between 625 and 1100 J/cm^2, roughness reduction remains greater than 80%.

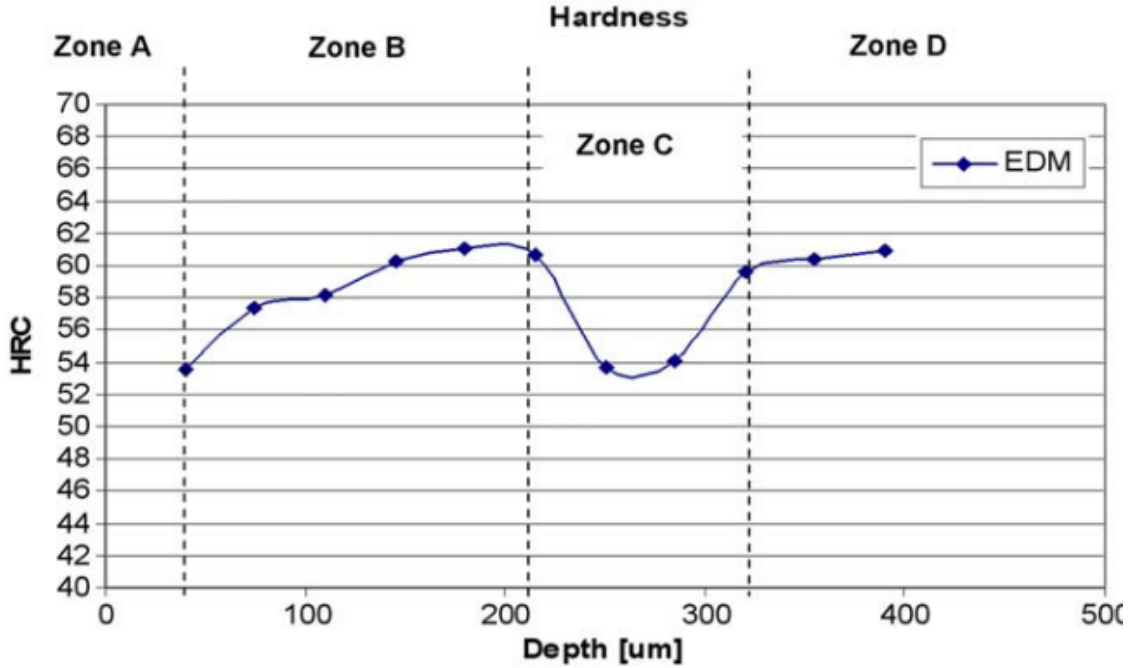

Fig. 18. Hardness values at different depths.

4. Discussion

In experimentation greater roughness reduction rates with higher productivity rates were achieved with the high power diode laser. This difference between CO_2 and diode lasers is due to the difference between the wavelength of the radiation, 906 nm for the diode laser and 10,600 nm for the CO_2 laser, and the material energy absorption difference for each wavelength.

The results shown in Fig. 4 are coherent with the expected values since, once an optimum value is reached, as the energy density is increased the melted layer thickness is greater, and lower reduction rates are therefore obtained. These results match the balance of SSM and SOM regimes, where once the melted layer thickness is greater than the peak–valley distance a melt pool is created, and a mass transfer takes place as a result of the convective currents caused by the thermal gradient. If the energy density is too high a volume increase may be appreciated in the polished area. This volume change is the result of mass transfer due to convective currents caused by the thermal gradient in the melt pool.

As mentioned in experimental tests, for the maximum roughness reduction rate of 87% of *Ra*, an energy density of 1,100 J/cm^2 was used (run 11 in Table 3). The metallurgical study for this energy density shows that melted layer thickness is close to 200 µm (Fig. 11), which is clearly over 34 µm, the peak–valley distance in the initial topography. In other words, for a ball-end mill surface with a Ø 16 mm diameter tool and a radial step of 1.5 mm on DIN 1.2379 tool steel, the optimum roughness reduction (over 80%) is obtained melting a layer thick enough to allow the peaks to be totally eliminated, and thin enough to prevent undulations due to mass transfers as a result of melt pool convective currents. In this case, even if the thickness of the melted material is six times the peak–valley distance, SSM is the dominant regime, and there is no undulation due to mass transfer of melted material.

4. Discussion

The regime transition between SSM and SOM depends, therefore, not only on the energy density and the thickness of the melted material, but also on the initial topography of the surface. Up to this point the tested surface had been a milled surface with an extremely large distance between two consecutive peaks (1.5 mm) in comparison with the peak–valley distance (34 μm). In this case, it was demonstrated that relatively high energy densities (melting up to 200 μm layer thickness) produce a dominant SSM regime.

5. Conclusion

This paper studies the application of laser polishing on DIN 1.2379 tool steel. Two different laser types were used in the preliminary tests—a 2.5 KW CO_2 laser and a 3.1 KW High-Power Diode Laser. High roughness reduction rates were obtained with both, over 75% using the CO_2 laser and over 80% with the diode laser. Although the roughness reduction rates obtained with both laser types are considerably high, the diode laser obtains the maximum reduction with lower energy density (1100 J/cm^2), with a wider spot for a greater area of processed surface per time unit.

Available online at www.sciencedirect.com
ScienceDirect
International Journal of Machine Tools & Manufacture 47 (2007) 2040–2050
INTERNATIONAL JOURNAL OF MACHINE TOOLS & MANUFACTURE DESIGN, RESEARCH AND APPLICATION
www.elsevier.com/locate/ijmactool

Laser polishing of parts built up by selective laser sintering

A. Lamikiz*, J.A. Sánchez, L.N. López de Lacalle, J.L. Arana

Department of Mechanical Engineering, University of the Basque Country, ETSII, c/Alameda de Urquijo s/n, 48013 Bilbao, Spain

Received 27 June 2006; received in revised form 22 January 2007; accepted 23 January 2007
Available online 20 February 2007

Laser polishing

LaserForm ST-100

Line polishing
Planar surface polishing
3D line polishing

1. Introduction

experimental results can be found. Furthermore, the quoted references indicate that there is a lack of a systematic and logical research for metal polishing.

The same manual abrasive techniques used for machined moulds are used to achieve the final finishing requirements in parts made by SLS, which can be time consuming and expensive job. Some investigations are addressed to

2. Laser-polishing fundamentals

Laser-polishing process is based on the melting of a microscopic layer and a fast re-solidifying of the melted material. The affected layer has to be deep enough to melt the roughness peaks, but it must not be deeper than the valleys. Therefore, the energy of the laser beam must be carefully controlled to melt just a microscopic layer. In Fig. 1, a scheme of the laser surface polishing process is presented.

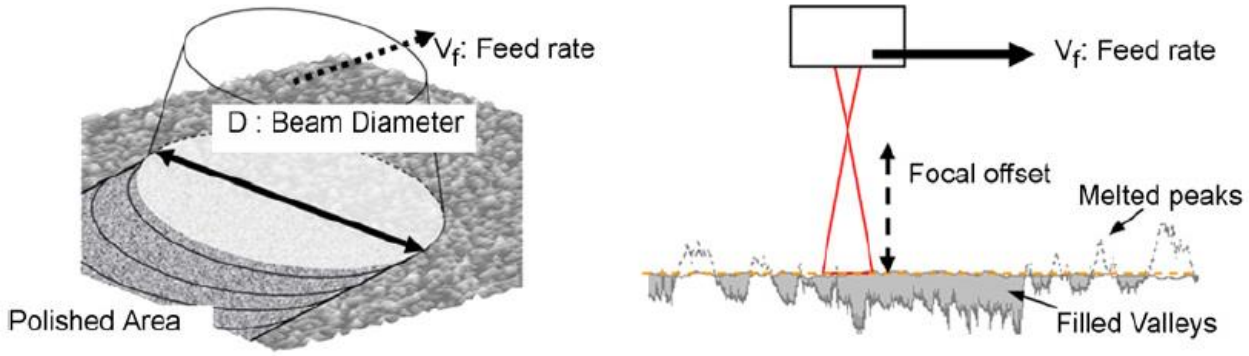

Fig. 1. Laser-polishing process scheme.

Nevertheless, the experiments show that both regimes are combined and final surface roughness depends on one dominant regime. If laser parameters are not accurately controlled, it is very difficult to predict which one will be the dominant regime. The most difficult parameter to control is the focal offset distance, measured from the laser focal point to the part surface, because it affects directly to the laser beam diameter. In the experimental set-up used in this work, an accurate control of the focal offset distance has solved this problem and no additional control has been used due to the simple tested geometries. However, for complex geometries, constant focal offset can be very difficult to control. This problem can be solved by using a system similar to the applied in industrial five-axis laser cutting systems. These machines install an additional axis and an inductive position sensor in the laser head; the additional axis is controlled by a closed-loop system that corrects the focal position of the laser instantaneously.

3. Laser-polishing Experimental tests and result discussion

In order to study the potential of the laser-polishing process, a set of experimental tests was carried out. In these tests a commercial alloy denominated LaserForm ST-100© was selected. This material is composed by approximately 60% of sintered AISI 420 stainless steel and 40% of infiltrated bronze; its mechanical and thermal properties are optimum for injection moulding applications. The test

The laser-polishing experiments have been carried out in a 2500 W CO_2 slab laser. The optic head was installed in a three-axis gantry machine with 10,000 mm min^{-1} maximum feed rate. The laser optics was originally designed for laser cutting operations; therefore, it has been possible to use the cutting assistance gas nozzle as a protecting gas flow to avoid metal oxidation of the part surface during polishing. The laser presents a Gaussian power density profile. Thus, the maximum energy density is focused on the center of the spot. The optimum beam profile for laser polishing processes is a top-hat profile that presents a large-constant energy peak. However, most of the RM machines use a CO_2 or a Nd:YAG laser with Gaussian profiles, in order to maximize the focusing of the laser beam and improve the resolution of the part details. Therefore, the experiments have been carried out taking into account the beam profile of most RM machines.

3. Laser-polishing Experimental tests and result discussion

The main process parameters are the laser beam feed rate, the laser power and the laser beam diameter. However, since the beam diameter is an indirect parameter, consequence of the focal offset distance, the controlled parameter in all tests has been the focal offset distance. The laser beam diameter was measured for each focal offset distance. The objective of the tests is to find a parameter combination to obtain the lower mean roughness (Ra) with the maximum feed rate and beam diameter. Therefore, the target is to increase the process productivity to the maximum value. Measured parameters have been the final topography of the polished surface, the mean roughness and the reduction index calculated as the relationship between the final and the initial roughness. These values have been obtained with a 3D profile and roughness measurement system.

3.1 Simple line polishing tests

First, to check the viability of the process, a series of simple line tests were carried out in planar surfaces. The test parts were manufactured by SLS with a layer thickness of 0.15 mm, resulting on an initial mean roughness of 7.5 μm Ra, which is a common value for sintered surfaces. Tested area was a LaserForm ST-100© 25 × 90 mm planar surface.

The experimental tests parameters are presented in Table 1. For all tests, argon was injected coaxially as shielding gas. The experimental results show that the optimum parameters were in the range of 4000–4500 J cm^{-2} energy density. Some dispersion on the results can be observed, which is logical taking into account that the initial surface topography is one of the main parameters (Fig. 3).

Table 1
Laser-polishing test parameters

Test no.	Power (W)	Feed (mm min^{-1})	Focal offset (mm)	Laser beam diameter (mm)	Energy density (J cm^{-2})	Roughness reduction (%)
1	600	2000	30	0.93	1935.48	74.8
2	900	1400	20	0.54	7142.86	0.9 (no coherent)
3	600	800	30	0.93	4838.71	62.8
4	1200	800	40	1.3	6923.08	59.6
5	1200	2000	30	0.93	3870.97	82.7
6	900	800	30	0.93	7258.06	73.3
7	900	1400	30	0.93	4147.47	78.8
8	600	1400	20	0.54	4761.90	78.6
9	900	800	40	1.3	5192.31	59.5
10	600	800	40	1.3	3461.54	52.0
11	1200	800	30	0.93	9677.42	71.3
12	900	1400	30	0.93	4147.47	80.2
13	1200	1400	30	0.93	5529.95	72.2
14	900	800	20	0.54	12,500.00	74.5
15	900	1400	30	0.93	4147.47	70.0
16	900	1400	30	0.93	4147.47	86.9
17	600	1400	30	0.93	2764.98	81.1
18	900	2000	30	0.93	2903.23	80.9
19	900	1400	30	0.93	4147.47	80.3
20	1200	1400	40	1.3	3956.04	78.8
21	900	2000	40	1.3	2076.92	75.6
22	1200	1400	20	0.54	9523.81	73.1
23	900	1400	40	1.3	2967.03	73.2
24	600	800	20	0.54	8333.33	79.5
25	600	2000	40	1.3	1384.62	72.7
26	900	2000	20	0.54	5000.00	77.4
27	600	2000	20	0.54	3333.33	77.4
28	1200	2000	40	1.3	2769.23	80.5
29	600	1400	40	1.3	1978.02	80.1
30	900	1400	30	0.93	4147.47	79.5
31	1200	800	20	0.54	16,666.67	57.6
32	1200	2000	20	0.54	6666.67	59.5

3.1 Simple line polishing tests

tests. The first appreciable result is that the resulting surface is much smoother than the initial one. The evaluation of the topography of Fig. 4 has to be made taking into account the different scales of both figures. On the other hand, as shown in the figure, the form profile of the test part is conserved. It denotes that the laser-polishing process does not affect to form deviations of the parts but only to surface roughness values.

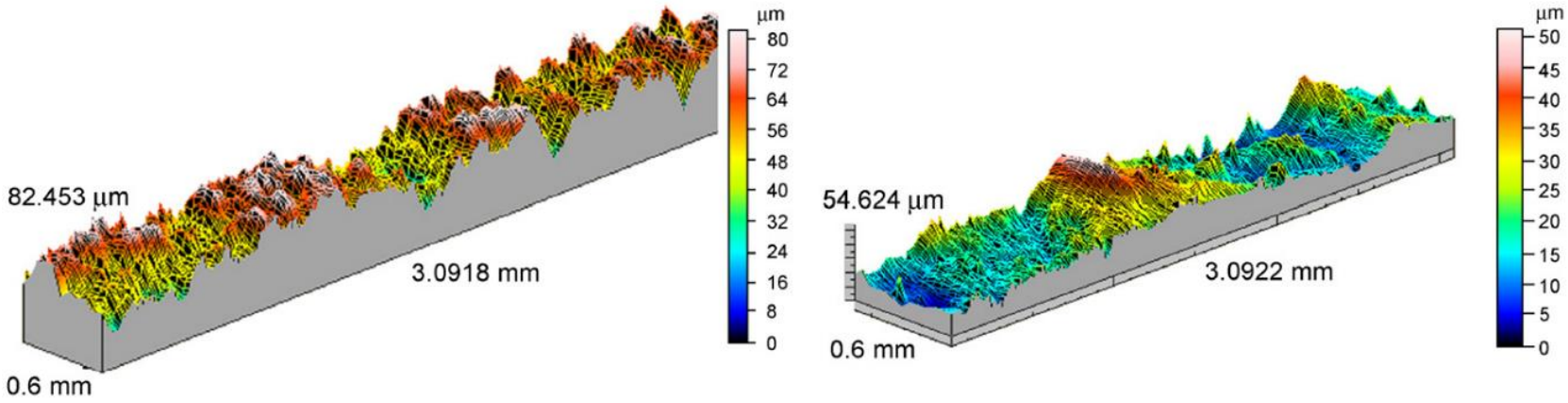

Fig. 4. Left: Original topography of the SLS test part. Right: final topography for a laser-polishing test for LaserForm ST-100©.

3.1 Simple line polishing tests

particular material composition. As it has been pointed above , LaserForm ST-100© is a mixture of stainless steel and bronze. The different melting points of these two materials can involve the melting of the bronze whereas the stainless steel is not affected. Therefore, if stainless steel matrix is melted, a deeper bronze layer is melted. Moreover, the best results were for more than 4000 J cm^{-2} energy density, much higher than the used for the DIN 1.2344 tool steel tests.

In order to evaluate the influence of all the parameters in the surface roughness, a design of experiments (DoE) was completed. The results of the DoE show the existence of an optimum roughness reduction for a given energy density.

criteria. Then, optimum parameters are shown in Table 2, considering maximum roughness reduction and maximum feed rate criteria.

In order to validate the DoE estimations, a new laser-polishing test set was compared with DoE predictions. In

Table 2
Optimum parameters from the design of experiments with LaserForm ST-100©

Laser power (W)	600
Laser feed rate V_f (mm min^{-}1)	1482.94
Distance (mm)	20
Resulting energy density (J cm^{-2})	4.580
Roughness reduction (%)	86.8

Table 3
Tests parameters and measured and DoE estimated roughness reduction

Test no.	Power (W)	Feed (mm min^{-1})	Focal offset (mm)	Laser beam diameter (mm)	Energy density (J cm^{-2})	Measured % reduction	DOE % estimated reduction	Difference (%)
1	1200	1400	27	0.85	6050.42	79.06	75.25	3.81
2	1200	1400	27	0.85	6050.42	75.85	75.25	0.60
3	1200	1800	27	0.85	4705.88	81.62	76.13	5.50
4	1200	1600	27	0.85	5294.12	66.45	76.38	−9.93
5	1200	2000	27	0.85	4235.29	82.05	74.48	7.57
6	800	1000	27	0.85	5647.06	74.57	77.49	−2.92
7	1000	1000	27	0.85	7058.82	76.71	74.77	1.94
8	800	800	27	0.85	7058.82	79.49	72.21	7.27
9	600	800	35	1.2	3750.00	86.11	71.71	14.40
10	850	1000	35	1.2	4250.00	83.33	77.11	6.22
11	850	1000	35	1.2	4250.00	86.54	77.11	9.43
12	900	1000	35	1.2	4500.00	89.74	76.53	13.21
13	950	1000	35	1.2	4750.00	89.32	75.75	13.56
14	750	1000	35	1.2	3750.00	76.71	77.66	−0.95
15	700	1000	35	1.2	3500.00	79.70	77.64	2.07
16	650	1000	35	1.2	3250.00	77.14	77.41	−0.27
17	600	1000	35	1.2	3000.00	83.33	76.97	6.36
18	600	1000	35	1.2	3000.00	85.04	76.97	8.07
19	550	1000	35	1.2	2750.00	83.33	76.34	7.00

3.1 Simple line polishing tests

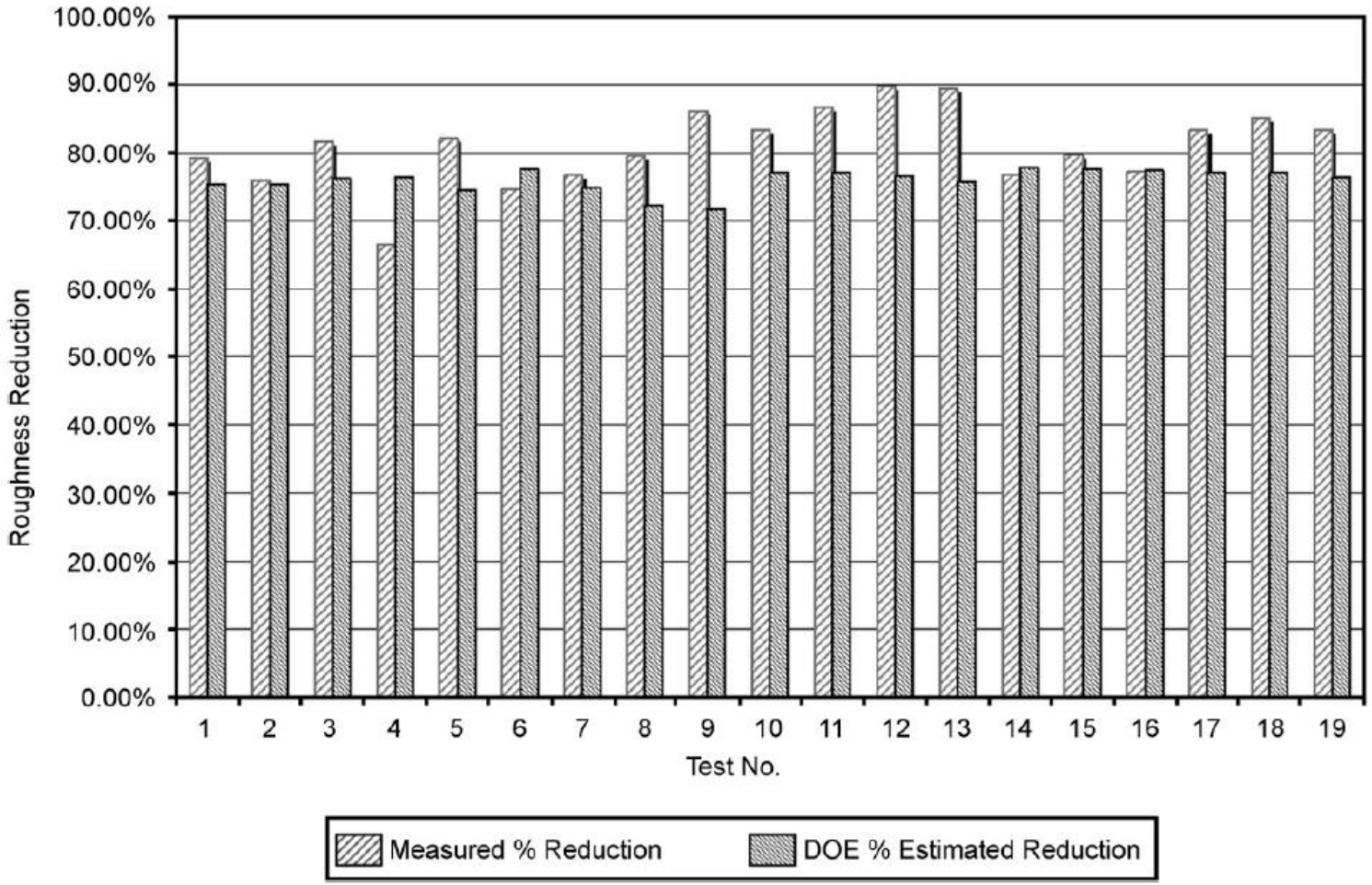

Fig. 6. Measured roughness reduction vs. DoE estimated values.

3.2 Planar surface polishing tests

Once the optimum parameters for linear polishing tests were found, horizontal surface polishing tests were performed. These tests were carried out by overlapping line tests on the surface. A new parameter, denominated overlap index (O_i), is introduced in this case. The overlap index measure the relative distance that a line overlaps with the last one. This parameter depends on two factors: the stepover distance and the width of the lines, which is equal to the beam diameter. A 100% overlap index indicates that the laser beam have polished the same previous one. If overlap index is 0% indicates that there is no any overlap between two consequent passes. In Fig. 7 a scheme of surface laser-polishing strategy and the calculation of overlap index are shown.

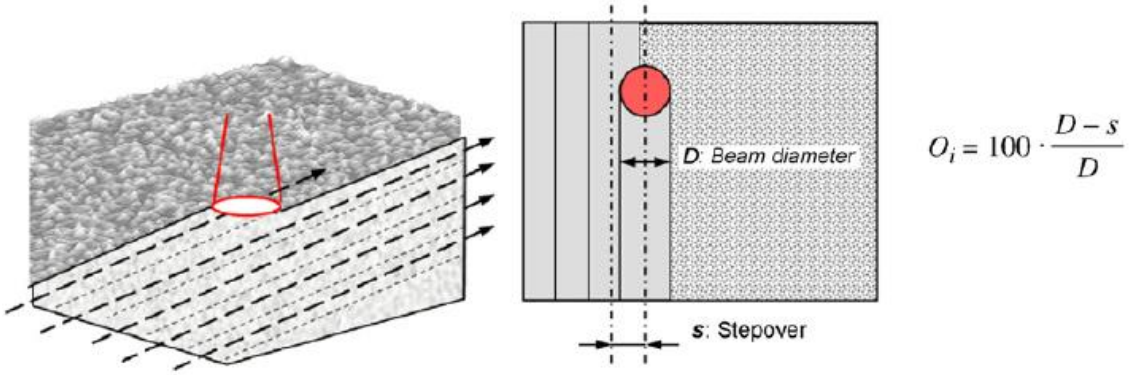

Fig. 7. Surface laser-polishing strategy.

Overlap between laser paths have to be enough to cover the gap between two lines, but too high values can lead on an excessive heat input on the same area, which can affect the final part. Thus, different overlap indexes have been tested, obtaining optimum results in the range from 15% to 30%. Taking into account that the beam diameter is about 0.8–2 mm, depending on the focal offset distance, the stepover value ranges between 0.7 and 1.5 mm.

3.2 Planar surface polishing tests

The tests included different overlapping indexes concluding that the best results were obtained for 25% with a reduction of 68.2% of roughness. The topographies before and after the polishing test are shown in Fig. 8, where roughness reduction can be also observed (noticing the different measurement scales). The measured mean roughness in the polished area was below 2.5 µm Ra and most of the areas present values below 1 µm. On the other hand, the measured topography presents an isotropic roughness, with similar roughness values in all directions, as it can be observed on the resulting topography, shown in Fig. 8. It is a well-known effect that the isotropic roughness improves the fatigue life of the parts since it avoids the nucleation of cracks.

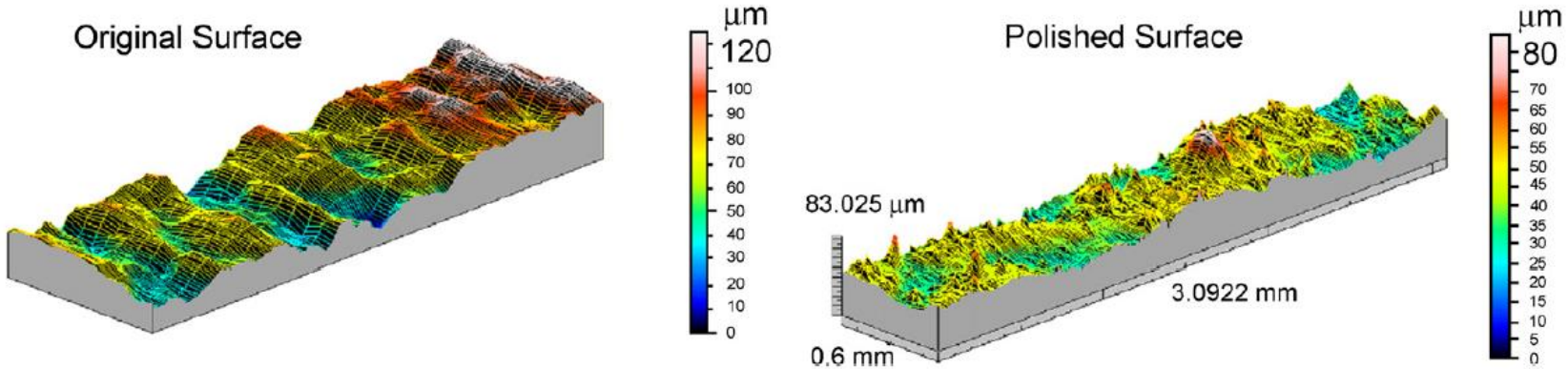

Fig. 8. Left: Initial surface topography. Right: test result for one laser-polished area.

3.3 Three dimensional polishing tests

tests were performed. A specific test part was designed to develop these 3D tests. Thus, a test part (see Fig. 9) with three different slopes (15°, 30° and 45°) was build-up by SLS.

Results show similar roughness reductions to the horizontal line tests. Final measured mean roughness is between 1.25 and 2.5 μm Ra. The same parameters obtained in linear tests were tested and the results show that optimum results were achieved with the same energy density.

It was also checked that the part shape profile does not change in any case. In Fig. 10, the initial roughness and a laser polishing resulting profile is shown. It can be observed that there is only a minimum variation in the part edges, whereas the roughness profile is much smoother than the initial one. The maximum measured deviation on the edges is 25 μm, while the surface reduction is 74.2%, similar to that obtained in horizontal tests.

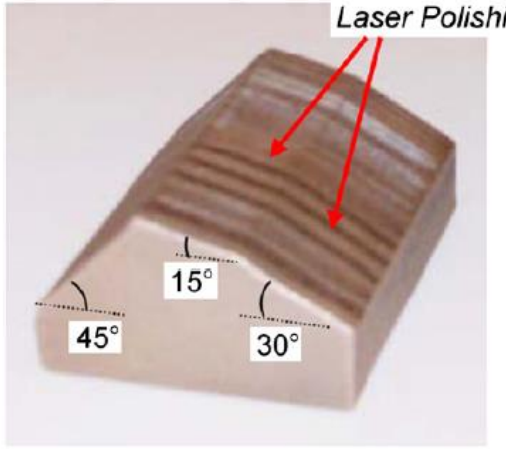

Fig. 9. 3D test part built up by SLS in LaserForm ST-100©.

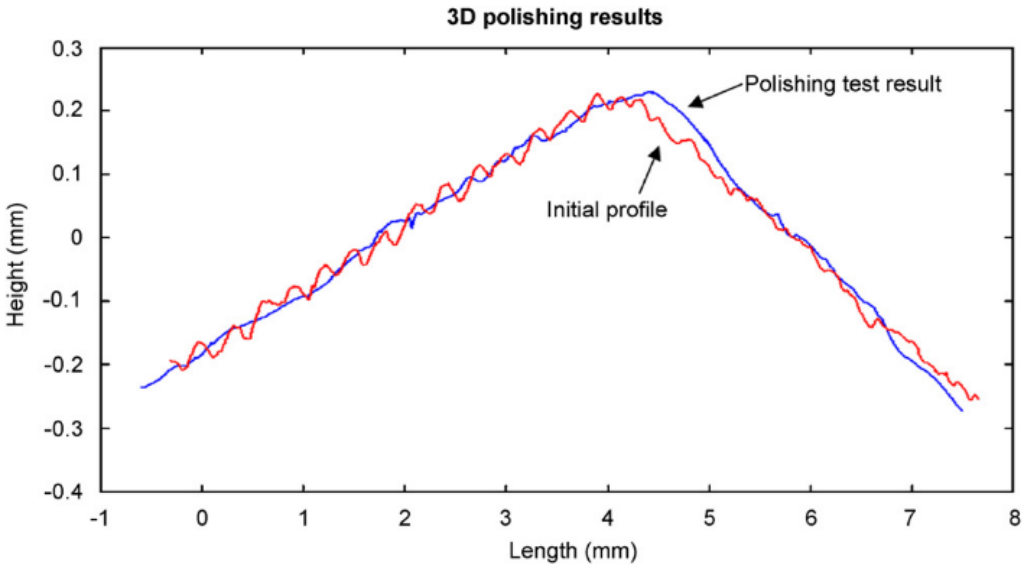

Fig. 10. 3D polishing results in LaserForm ST-100©.

3.4 Results and disscussion

Experimental results for laser polishing show that the mean roughness decreases for all the tested cases. Experimental results show that the most important parameter is the energy density. On the other hand, the final surface roughness depends on the initial surface roughness, thus, the surface roughness reduction presents some dispersion due to different surface topographies of the tested surfaces.

Tests show reductions upto 76% with no form profile deviations. These reductions show that the process is able to improve the surface roughness considerably. However, the minimum measured mean roughness was 1.49 μm Ra. This value cannot be considered as a polished surface and final hand polishing should be done to reduce this value below 1 μm. The results can be explained at the view of the material composition. The necessity to melt two different materials with different melting points, forces to increase the energy density. Thus, the melted layer is deeper and the final roughness reduction is lower than the expected. This hypothesis is coherent with the presence of the SOM regime.

4. Integrity of the laser polished surfaces

One of the most important aspects to be controlled is the influence of the process in the polished surface properties. Some polishing techniques induce high residual stress which can lead to cracking and fatigue failure. On the other hand, laser processes involve surface melting and re-solidification. Therefore, some heat affected zone (HAZ) will be present and must be analyzed in order to control the material behaviour.

Although there are more potential applications, laser polishing of sintered parts has been focused basically for small plastic injection moulds or inserts. In these parts, the most common failure cause is thermal fatigue and abrasion. Thermal fatigue can be reduced with high

The analysis results show that three different areas can be distinguished in the laser polished zone. First, denominated as Area 1, the initial substrate material, which is a stainless steel bounded particles matrix with bronze infiltration. Despite the bronze infiltration, some porosity can be observed in this area due to the sintering process. This porosity affects significantly to mechanical properties of the material. The second area (Area 2) is located surrounding the polished surface. Its composition is almost 100% AISI 314 stainless steel, with no bronze presence. This area is harder than the previous one because there is only stainless steel and, due to the re-solidification process, the material is much more homogeneous than the sintered one. Finally, the third area or Area 3 is the polished area and is located on the part surface. It is composed of a mixture of stainless steel and bronze, with a higher proportion of bronze. The high proportion of bronze is due to an exudation of this alloy from the stainless steel matrix. The resulting material is much more homogeneous than the substrate material and no porosity is appreciated. On the other hand, the polished layer material is harder than the substrate, although it is not as hard as the stainless steel layer. This effect will improve wear resistance of the surface. In Fig. 11 two different laser-polishing test sections

Table 4
Laser-polishing test parameters for LaserForm ST-100©

Test conditions	Test A	Test B
Laser power (W)	1100	800
Laser feed rate V_f (mm min^{-1})	800	1100
Focal offset distance (mm)	40	30
Shielding gas	Argon	Argon

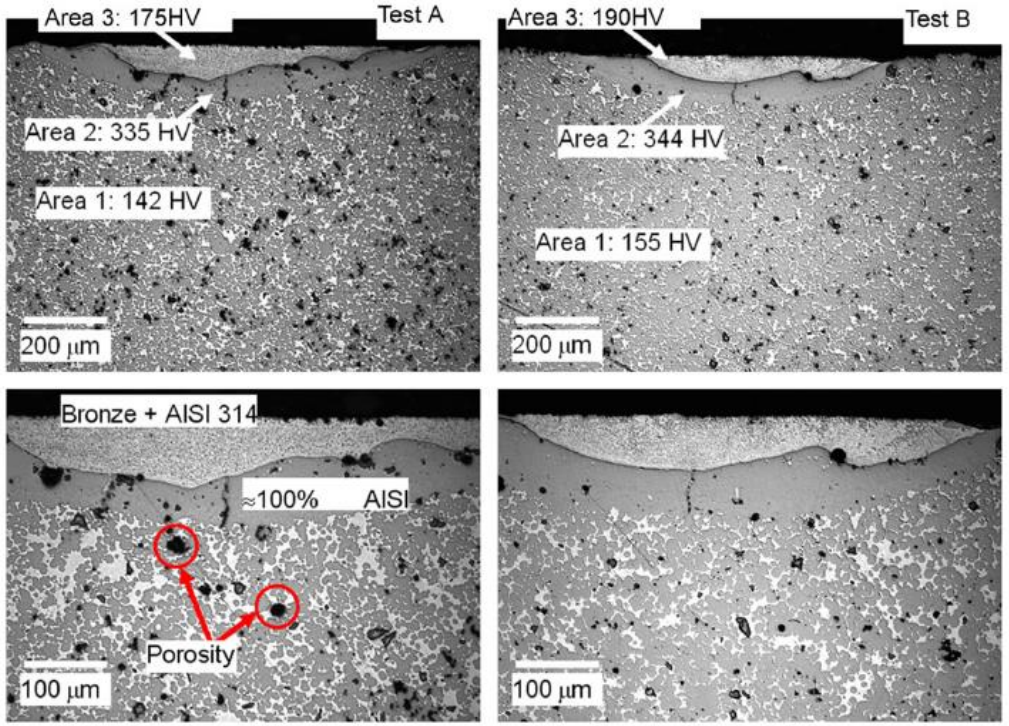

Fig. 11. LaserForm ST-100© laser polished line sections for two tests.

5. Conclusion

In the work presented here, a laser-polishing process for metallic sintered parts by SLS has been described. The results show clear roughness reductions for a commercial material denominated LaserForm ST-100© which consists on sintered AISI 420 stainless steel infiltrated with bronze. The measured reductions are up to 80% reductions in Ra parameter. That means a final roughness of 1.2–1.3 μm Ra whereas the initial surface roughness was in the range of 7.5 μm Ra.

the optimum. Therefore, energy density is the most important parameter of the process. Thus, once evaluated the optimum energy density, the optimal parameters are those that optimize feed and spot diameter, in order to obtain the maximum productivity. The experimental results also conclude that the rougher the original surface, the more effective the process is.

Experimental results show that optimum overlapping index is about 15–30%. Finally, a 3D test part, shaped by three

Metallurgical analyses show that the heat affected zones do not present cracks or porosity. It can be concluded that laser affected areas present a more homogeneous composition than the initial ones. On the other hand, resulting

Thin Solid Films 518 (2009) 1072–1078

Contents lists available at ScienceDirect

Thin Solid Films

journal homepage: www.elsevier.com/locate/tsf

Laser patterning with beam shaping on indium tin oxide thin films of glass/plastic substrate

Ming-Fei Chen [a,*], Wen-Tse Hsiao [a], Yu-Sen Ho [a], Shih-Feng Tseng [b], Yu-Pin Chen [c]

[a] *Department of Mechatronics Engineering, National Changhua University of Education, Changhua, 50058, Taiwan*
[b] *System Control and Integration Division, Instrument Technology Research Center, National Applied Research Laboratories, Hsinchu, 30076, Taiwan*
[c] *PCB Department, Tongtai Machine & Tool CO., LTD, Kaohsiung, 82151, Taiwan*

ITO laser patterning

Beam shaping

ITO / glass **ITO / PC(Polycarbonate)**

Line patterning

- Laser power
- Repetition rate
- Table speed
- Complex electrode patterning

1. Introduction

patterning process is required. The traditional patterning processes needs several steps, including (1) photoresist coating, (2) soft bake, (3) exposure, (4) lithography, (5) hard bake, (6) etch and (7) photoresist stripping. In wet chemical etch process exist for the fixable plastic substrates. Several disadvantages, include higher absorption coefficient of water, lower corrosion resistance of acid and higher thermal expansion coefficient. Therefore, a new method, the laser direct writing method, is purposed to reduce the high investment of semiconductor lithography process equipment, and to decrease the chemical harm to the environment.

elements, spherical-surface lens and diffraction lens [10]. In order to obtain the uniform depth of the polymer surface on the exposed region, Corbett [12] proposed that the Gaussian beam shaped to the

2. Experimental setup

Laser electrode patterning system consists of a UV laser source, an optical system, a feeding system, a scanner unit and a PC-based controller. A wavelength of 355 nm can be obtained by laser oscillator with triple harmonic generation. The output average power of the laser source can be adjustment from 0.07 W to 3.33 W. The range of

pulse repetition rates can be adjusted from 1 kHz to 10 kHz . The pulsewidth and laser pulse duration of 35 ns and 1000 μs, respectively. In addition, the accumulated energy for different repetition rate from 9.9 mJ/cm^2 to 651 mJ/cm^2 with laser output power of 0.07 W and 0.46 W. In the optical path, laser beam passes though a beam expander, aperture, beam splitter, mirrors, beam shaper component and scanning system. A laser beam for micropatterning ITO thin films

used in the experiment are given in Table 1. The polished soda–lime glass and polycarbonate (PC) plastics substrates with thickness of 1.1 mm and 1 mm, respectively. The deposition method by DC sputtering process to coated indium tin oxide (ITO) thin films with thickness of about 400 nm. The roughness of the coated ITO thin films with different types of substrates can be shown in Fig. 1(a) and (b).

3. Results and discussion

ITO/glass and ITO/PC. In the line patterning process, controlling x–y axes stages to fabricate electrode line patterning with the average power of 0.07 W and 0.46 W. The repetition rate varied from 1 kHz to 10 kHz and stages feeding speed were fixed at 40 mm/s. Fig. 4(a)

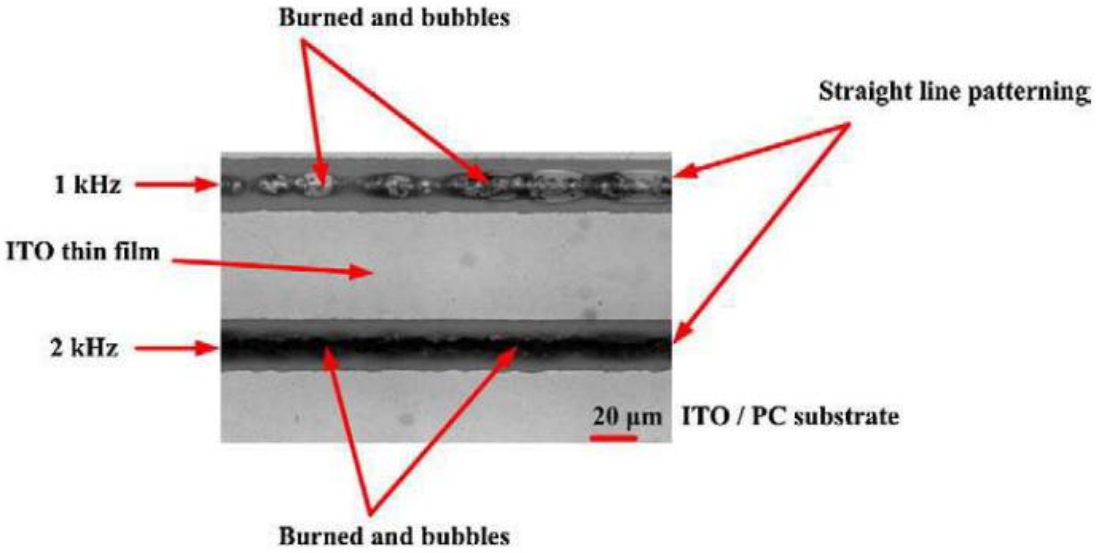

This is because the accumulated energy density and higher pulse repetition rate could not ablate the ITO thin films. Furthermore, there was a 10× magnification optical microscope image of line patterning as shown in the Fig. 4(b), (c) and (d). The burned and bubble phenomenon of the ITO thin films and inner substrates are observed at the pulse frequency of 1 kHz and 2 kHz. Laser with lower pulse frequency accumulates more energy on the power to lead to damaged substrates or affect its performance. Non-continuous line patterning process appeared at the pulse frequencies of 5 kHz and 6 kHz, the line pattering on ITO thin films could not totally isolate electric conductivity.

3. Results and discussion

Similarly, Fig. 5(a) shows the straight line patterning experimental results using an optical microscope. We use the 0.46 W laser power and the different pulse repetition rates from 1 kHz to 10 kHz to expose ITO thin films. In this case study, the pulse energy can be adjusted from 651 mJ/cm^2 to 65 mJ/cm^2. The laser output power of 0.46 W and pulse repetition rate of 6 kHz as shown in Fig. 5(a) has a good quality for line patterning. In the line patterning process, there are not only completely ablated thin films but also those without damaged or burned substrates under the different pulse repetition rates. The larger-scale inspection of the line pattering on ITO thin films was shown in Fig. 5(b), (c), (d), (e) and (f). Fig. 5(b), (c) and (d) reveals

the burned-out, bubble and damaged substrates at 1 kHz, 2 kHz, 3 kHz, 4 kHz and 5 kHz with pulse energies of 651 mJ/cm^2, 325 mJ/cm^2, 216 mJ/cm^2, 163 mJ/cm^2, and 130 mJ/cm^2, respectively. From the results of the damaged substrates by the line patterning process, it shows that pulse repetition rates of 6 kHz and 7 kHz, laser power of 0.46 W with pulse energies of 108 mJ/cm^2 and 93 mJ/cm^2, and feeding speed of 40 mm/s can obtain a much superior quality.

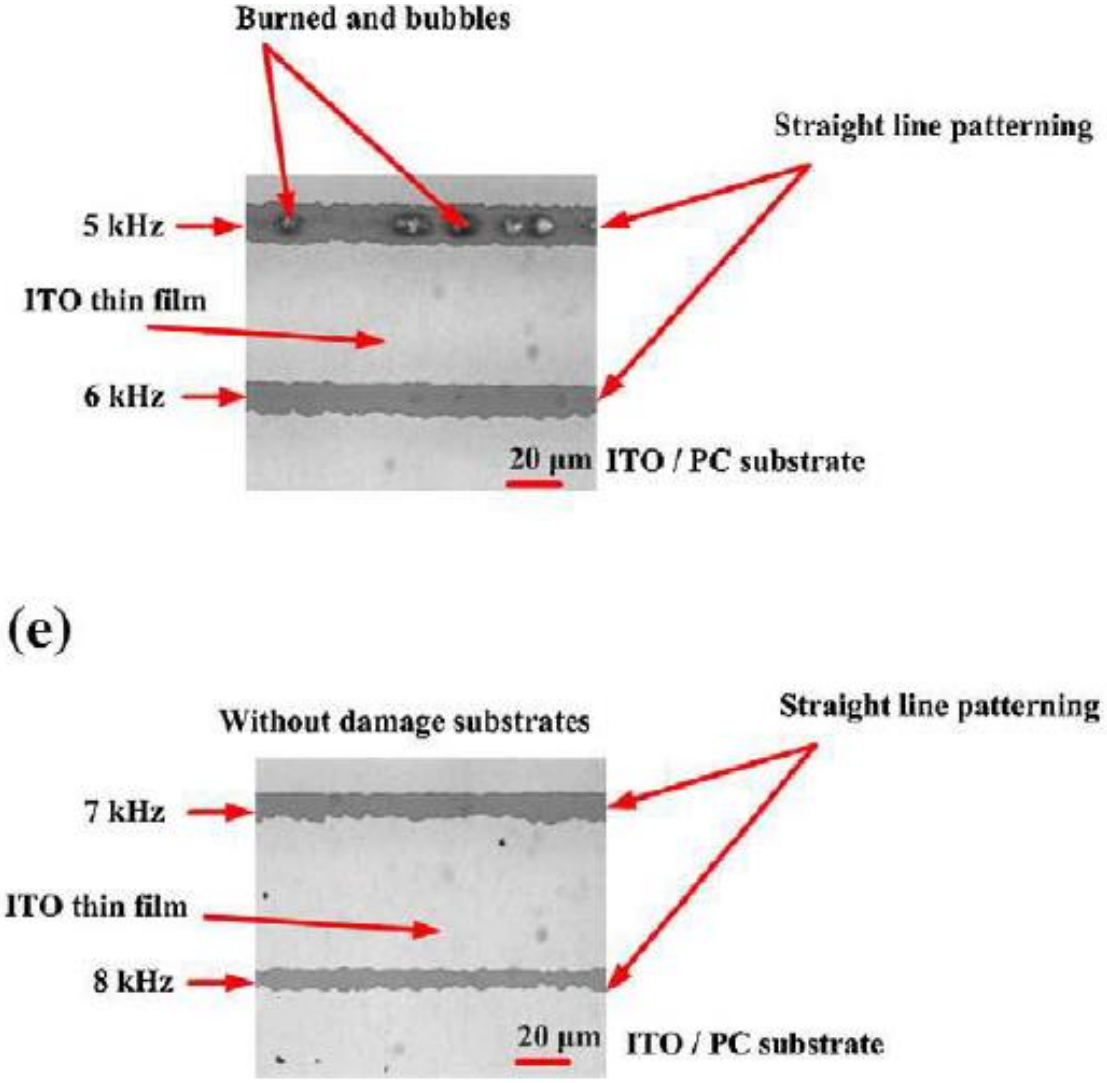

3. Results and discussion

process. Fig. 7(a) shows the designed complex electrode patterning. The results of complex patterning on ITO/PC substrate are shown in Fig. 7(b). The size of the electrode patterning area was about 6 mm × 9 mm. Both the lines and spaces are 600 μm. The patterning region did not damage the substrate by optical microscope measurements. Additionally, the sharp corner of the etched pattern in high magnification is shown in the Fig. 7(c). The dark part was the removed portion of the patterned area and the bright part was without the patterned area on ITO thin films. The boundary between the dark and bright parts is clearly observed and the etched process is conducted uniformly. Fig. 8 shows the result of partial complex circuit patterned on ITO/glass substrate by SEM. The laser power was 0.46 W, the laser pulse repetition rate was 8 kHz with pulse energy of 81 mJ/cm^2 and the pulse duration of 1000 μs. The complex patterned line-width was about 100 μm. In this complex patterning case, there is a heat affect zone (HAZ) as shown in Fig. 8 light part region and some particle residual around the electrode patterning, and those results lead to a worse quality in the electronic characteristics and transmission efficiency of light.

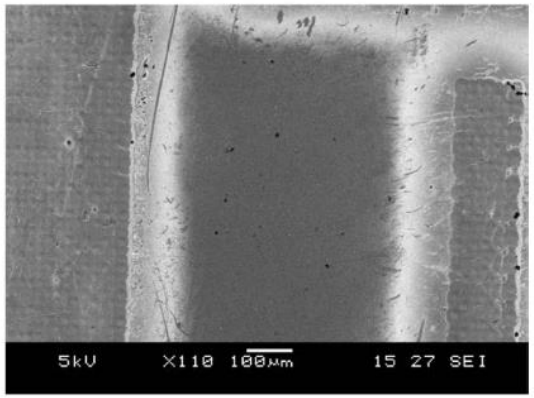

Fig. 8. SEM micrograph of complex electrode patterning on ITO/glass substrate.

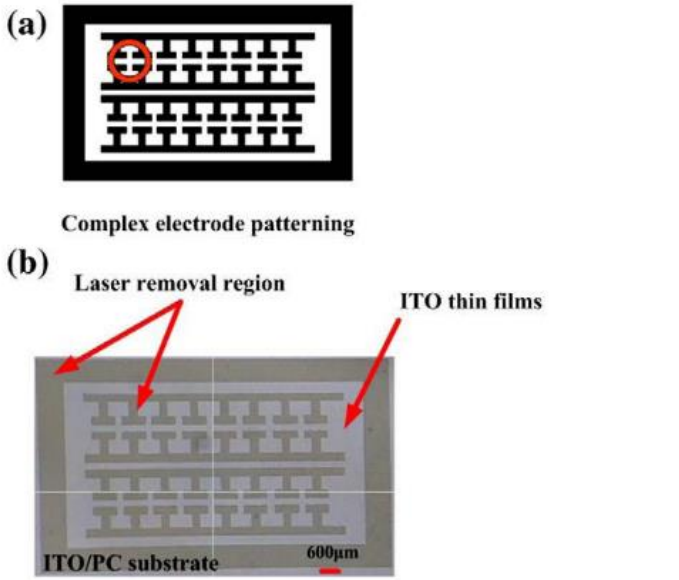

Fig. 7. Circuit patterns ablated by UV laser processing system on ITO/PC substrate.

4. Conclusions

This research has successfully investigated that using laser processing can selectively remove ITO films for isolated line patterning and complex electrode patterning on glass and plastic substrates. Some experimental parameters such as the laser power, the laser pulse repetition rate, the pulse energy and the feeding speed of movable stages have been discussed. By the optical microscope and scanning electron microscope, the burning, micro-crack, damaged substrates, non-continuous isolate line, heat affect zone and some particle debris of material surface and substrates were observed. Additionally, the complex electrode patterning morphology was uniform, smooth and without damage to substrates of laser electrode patterning. After laser patterning, some particle debris occurred around the electrode patterning and that phenomenon lead to a worse quality in the drift characteristics of electronic and the transmission efficiency of light.